

## DYNAMIC MODELING OF FUNCTIONALLY GRADED BEAMS UNDERGOING MOBILE MASS

Abbes Elmeiche<sup>1</sup>, Mohamed Bouamama<sup>2✉</sup>, Abdelhak Elhannani<sup>1</sup>, Azzeddine Belaziz<sup>2</sup>,  
Abderazek Hammoudi<sup>2</sup>

<sup>1</sup>Laboratory of solids and structures mechanics, Faculty of Technology, University of Sidi-BelAbbes, (22000),  
Algeria

<sup>2</sup>Mechanics Research Center (CRM), BP N73B, Ain El Bey, 25021 Constantine, Algeria

✉ bouamamamohameddoc@gmail.com

**Abstract.** In this paper, the dynamic modeling of functionally graded beams subjected to a mobile mass is studied using modal analyzes. The material properties are assumed to vary continuously in the transverse direction according to an exponential law. A new simple shear deformation beam theory (SFPSDBT) has been formulated and employed in the study, taking into account the effect of the material inhomogeneity and as well the inertia of moving mass. The governing equations are derived using Hamilton's principle combined with a Galerkin weighted residual approach. The forced dynamics are solved by using the implicit Newmark method via the MATLAB program. Detailed analysis is performed to determine the impact of; material properties distribution, charging speed, the inertia of traveling mass, slenderness ratio, and mass weight on the dynamic responses. We can state that the above-mentioned effects should be considered in mathematical modeling, as they play a very important role in the forced vibration of functionally graded beams undergoing mobile mass.

**Keywords:** dynamic modeling, FG beams, mobile mass, SFPSDBT, Galerkin approach, charging speed, modal responses.

**Acknowledgements.** No external funding was received for this study.

**Citation:** Elmeiche A., Bouamama M., Elhannani A., Belaziz A., Hammoudi A. Dynamic modeling of functionally graded beams undergoing mobile mass // Materials Physics and Mechanics. 2022, V. 48. N. 1. P. 91-105. DOI: 10.18149/MPM.4812022\_8.

### 1. Introduction

Better understanding the vibration behavior of a structure leads to better design to prevent the designed structures resonates and suffering damage. Moreover, the influence of various parameters on the vibration behavior, such as the section and the length, the damping, as well as the materials used, will be better understood. The optimization of the design can result, for example, by reducing the weight or increasing stiffness and even improved vibration damping [1].

The vibratory analysis of structural elements is an important study to solve engineering problems.

Hence, the now ledge of natural frequencies allows the designer to avoid the resonance phenomena appearing near the natural frequencies [2].

Functionally graded materials (FGM) are a new class of composite materials whose microstructure and composition varied gradually and continuously with a position to optimize the mechanical and thermal performance of the structure they constitute. This material is widely used in many structural fields such as; the fields of aviation, nuclear, civil, and automotive. Several researchers have been studied the mechanical and thermal behavior of FGM structures [3-15].

To evaluate the vibratory characteristics in the design of products, structures, and mechanical parts. The engineer needs analytical models that they allow to simulate both the geometric shape of objects (shape and position) and dynamic behavior laws modeled structures. These laws are more or less faithful to what is happening in reality. In addition, dynamic systems are often subjected to external time-dependent forces leading to forced vibration whose amplitude depends on the frequency ratio. If the frequency of the external force coincides with one of the natural frequencies of the element under consideration, such as beams, plates, and shells; resonance occurs which results in dangerously large oscillations. Nami and Janghorban [13] present the resonance behaviors of functionally graduated micro/nanoplates using Kirchhof's plate theory, which investigates the effects of the gradient parameter, the aspect ratio, and the nonlocal parameter. Khebizi et al. [16] study the impact of materials on the parametric resonance of FG plates.

Many projects have been found in the literature on the static and dynamic study of FGM beams. Khebizi et al. [17] were using the theory of Saint-Venant 3D beams to study the mechanical behavior of FGM beams. Majak et al. [18] carried out a free vibration analysis of nano-beams in functional gradient materials in which they evaluated the Haar wavelet method. Garg et al. [19] did a comparative study of different FGM laws using the refined layer beam theory. Lee et al. [20] analyze the free vibrations of Euler-Bernoulli FGM beams using an exact transfer matrix expression. Moreover, other researchers [21-23] studied the dynamic stability of FGM beams. The study of the forced vibratory behavior of the FGM beam has also attracted research-intensive interest. For example, Simsek and Kocaturk [24] studied the free and forced vibration of functionally graded beams subjected to moving harmonic load concentrated, based on the classical theory of Euler-Bernoulli. Almbaidin and Abu-alshaukh [25] used a model derived fractional-Caputo Fabrizio to analyze the speed of the oscillator, the rank order of materials, the damping ratio, and the fractional drift simply supported FGM beam under an oscillator moving. Elmeiche et al. [26] carried out an analysis of the dynamic behavior of nano-beams in functional gradation materials (FGM) excited by a moving concentrated load, based on the theory of nonlocal elasticity, taking into account the effect of shear strain beams. Nguyen et al. [27] studied the dynamic response of non-uniform porous FGM beams subjected to dynamic forces; they assume that the cross-section of the beam varies longitudinally in the width direction by a linear or quadratic function.

The main objective of this research is to present a model which characterizes the forced dynamic behavior of a simply supported functionally graded beam undergone by a moving mass. Based on the new Simple Fifth order Polynomial Shear Deformation Theory (SFPSDBT), the equations of motion are derived using Hamilton's principle combined with a weighted residual Galerkin approach. MATLAB software is adopted to solve the modal responses of the vibratory system via Newmark's implicit method. Furthermore, the distribution of material properties, velocity, and inertia of the mobile mass, slenderness ratio, and mass weight on the dynamic deflection of functionally graded beams are analyzed in detail.

## 2. Dynamics modeling

Consider a simply-supported FG beam of length  $L$ , uniform thickness  $h$  and width  $b$ , subjected to a transverse mass ( $M$ ) which moves by a transient motion defined by a constant

velocity ' $v_M$ ' see Fig. 1. The upper and lower faces of the beam are at  $z=\pm h/2$ . The Functionally Graded Material (FGM) varies continuously due to the gradual change in the volume fraction of the constituent materials, generally in the thickness direction. It is assumed that the beam has a linear elastic behavior with the Cartesian coordinate system (o, x, y, z).

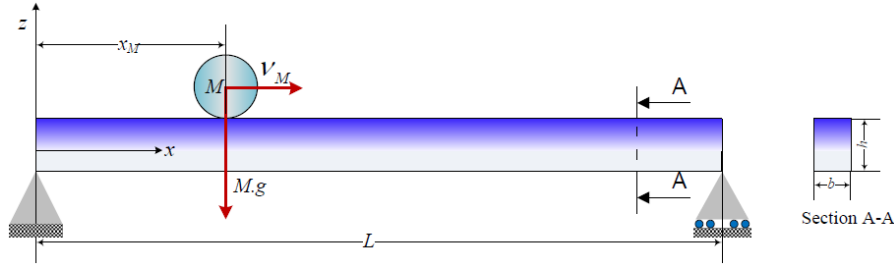


**Fig. 1.** FGM beam under dynamic moving mass

### 3. Kinematics

Based on the third-order shear deformation beam theories, the displacements coordinates of any point of the beam are given as:

$$\begin{cases} u(x, z, t) = u_o(x, t) - z w_{o,x}(x, t) + f(z) \cdot \phi_o(x, t) \\ w(x, z, t) = w_o(x, t) \end{cases} \quad (1)$$

$u_o(x, t)$  and  $w_o(x, t)$  are the displacement components in the middle of the section and on the mean line of the beam respectively along the (x) and (z) axes.  $\phi_o(x, t)$  is the distortion, also measured on the middle line of the beam. (t) represent the time index. In the small disturbances hypothesis, the strain-displacement relations of the high order beam theories are written as follows:

$$\begin{cases} \epsilon_{xx} = \frac{\partial u(x, z, t)}{\partial x} = \frac{\partial u_o(x, t)}{\partial x} - z \frac{\partial^2(w_o(x, t))}{\partial x^2} + f(x) \frac{\partial \phi_o(x, t)}{\partial x} \\ \epsilon_{yy} = \frac{\partial v(x, z, t)}{\partial y} \\ \epsilon_{zz} = \frac{\partial w(x, z, t)}{\partial z} = \frac{\partial w_o(x, t)}{\partial z} \\ \gamma_{xy} = \frac{\partial u(x, z, t)}{\partial y} + \frac{\partial v(x, z, t)}{\partial x} \\ \gamma_{xz} = \frac{\partial u(x, z, t)}{\partial z} + \frac{\partial w(x, z, t)}{\partial x} = g(z) \phi_o(x, t) \\ \gamma_{yz} = \frac{\partial v(x, z, t)}{\partial z} + \frac{\partial w(x, z, t)}{\partial y} = \frac{\partial w_o(x, t)}{\partial y} \end{cases} \quad (2)$$

The new shear stress distribution function is defined by a Simple Fifth-order Polynomial (SFP) such as:

$$f(z) = z \left[ 1 - \frac{3}{2} \left( \frac{z}{h} \right)^2 + \frac{2}{5} \left( \frac{z}{h} \right)^4 \right], \quad (3)$$

$$g(z) = 1 - \frac{9}{2} \left( \frac{z}{h} \right)^2 + 2 \left( \frac{z}{h} \right)^4, \quad (4)$$

where  $f(z)$  is the shape function that characterizes the transverse shear strain and shear stress through the depth of the beam.  $g(z)$  is the derivative of transverse shear functions along the thickness direction (z).

#### 4. Constitutive Equations

In this study, the material properties (Young's modulus  $E$ , Poisson's ratio  $\nu$  and density  $\rho$ ) vary continuously in the thickness direction " $h$ " of the beam according to exponential law (E-FGM). Many researchers use the exponential function to describe the material properties of materials, for the sake of simplicity. The exponential function is found by Delale and Erdogan [28]:

$$P(z) = P_t \exp(-\delta_0(1 - 2z/h)), \quad \delta_0 = \frac{1}{2} \ln \left( \frac{P_t}{P_b} \right), \quad (5)$$

$P(z)$  denotes the effective material properties.  $P_t$  and  $P_b$  denote the variable values at the top and bottom of functionally graded beams, respectively. The variation profile of material properties through the thickness of the beams E-FGM is shown in Fig. 2. Remarkably, the variation of material properties is done using a single function that dominates the distribution of materials in the Exponentially Functionally Graded beams (E-FGM).

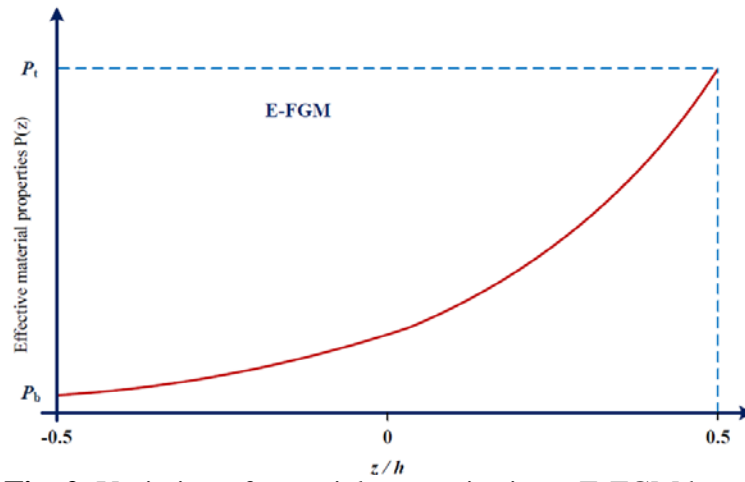


**Fig. 2.** Variation of material properties in an E-FGM beam

The stress-strain relations of the functionally graded beam can be written as:

$$\begin{bmatrix} \sigma_{xx} \\ \sigma_{yy} \\ \sigma_{zz} \\ \sigma_{xy} \\ \sigma_{xz} \\ \sigma_{yz} \end{bmatrix} = \begin{bmatrix} Q_{11} & Q_{12} & Q_{13} & 0 & 0 & 0 \\ Q_{21} & Q_{22} & Q_{23} & 0 & 0 & 0 \\ Q_{31} & Q_{32} & Q_{33} & 0 & 0 & 0 \\ 0 & 0 & 0 & Q_{44} & 0 & 0 \\ 0 & 0 & 0 & 0 & Q_{55} & 0 \\ 0 & 0 & 0 & 0 & 0 & Q_{66} \end{bmatrix} \begin{bmatrix} \varepsilon_{xx} \\ \varepsilon_{yy} \\ \varepsilon_{zz} \\ \gamma_{xy} \\ \gamma_{xz} \\ \gamma_{yz} \end{bmatrix} \quad (6)$$

The axial force ( $N^c$ ), bending moments ( $M^c$  and  $M^{sd}$ ) and shear force ( $Q^{sd}$ ) are defined by:

$$\begin{cases} N^c = \int_S \sigma_{xx} . dS \\ M^c = \int_S \sigma_{xx} . z . dS \\ M^{sd} = \int_S \sigma_{xx} . f(z) . dS \\ Q^{sd} = \int_S \tau_{xz} . g(z) . dS \end{cases} \quad (7)$$

Exponent (c) indicates conventional theories of classical beams, while exponent (sd) are additional quantities incorporating the effects of shear strain. The constitutive equations for FGM beam forces and strains are obtained by using Equations 2, 7, and 6:

$$\begin{bmatrix} N^c \\ M^c \\ M^{sd} \end{bmatrix} = \begin{bmatrix} A_{11} & B_{11} & E_{11} \\ & D_{11} & F_{11} \\ sym. & & H_{11} \end{bmatrix} \begin{bmatrix} u_{0,x} \\ -w_{0,xx} \\ \phi_{0,x} \end{bmatrix} \text{ and } Q = [A_{55}][\phi_0]. \quad (8)$$

The extensional, coupling, bending, and transverse shear stiffness are given as follows:

$$(A_{11}, B_{11}, D_{11}) = b \int_{-\frac{h}{2}}^{+\frac{h}{2}} Q_{11} (1, z, z^2) dz, \quad (9)$$

$$(E_{11}, F_{11}, H_{11}) = b \int_{-\frac{h}{2}}^{+\frac{h}{2}} Q_{11} f(z) (1, z, f(z)) dz, \quad (10)$$

$$A_{55} = b \int_{-\frac{h}{2}}^{+\frac{h}{2}} Q_{55} [g(z)]^2 dz, \quad (11)$$

where the reduced elastic constants are defined by:

$$Q_{11}(z) = \frac{E(z)}{(1 - \nu(z)^2)}; Q_{55}(z) = \frac{E(z)}{2(1 + \nu(z))}. \quad (12)$$

## 5. Variational formulations

To derive the equations of motion, the equilibrium equations will be obtained from the Hamilton principle:

$$\delta \int_{t_1}^t (\Delta - \square - \Pi) dt = 0. \quad (13)$$

The virtual strain energy  $\delta \Gamma$  is given by:

$$\delta \Gamma = \int_V (\sigma_{xx} \delta \epsilon_{xx} + \tau_{xz} \delta \gamma_{xz}) dV = \int_0^L (N^c \delta u_{0,x} - M^c \delta w_{0,xx} + M^{sd} \delta \phi_{0,x} + Q^{sd} \delta \phi_0) dx. \quad (14)$$

The variation of the kinetic energy  $\delta \Delta$  is obtained as:

$$\begin{aligned} \delta \Delta &= \int_V \rho(z) (\dot{u} \delta \dot{u} + \dot{w} \delta \dot{w}) dV \\ &= \int_0^L (I_1 \ddot{u}_0 - I_2 \ddot{w}_{0,x} + I_3 \ddot{\phi}_0) \delta u_0 dx - \int_0^L (I_2 \ddot{u}_0 - I_4 \ddot{w}_{0,x} + I_5 \ddot{\phi}_0) \delta w_{0,x} dx \\ &\quad + \int_0^L (I_3 \ddot{u}_0 - I_5 \ddot{w}_{0,x} + I_6 \ddot{\phi}_0) \delta \phi_0 dx + \int_0^L I_1 \ddot{w}_0 \delta w_0 dx. \end{aligned} \quad (15)$$

Such as:

$$(I_1, I_2, I_3, I_4, I_5, I_6) = \int_S \rho(z) (1, z, f(z), z^2, zf(z), f(z)^2) dS. \quad (16)$$

The virtual potential energy  $\delta \vartheta$  of the moving masse can be expressed as:

$$\delta \vartheta = - \int_0^L P(x, t) \delta w_0 dx. \quad (17)$$

The moving mass  $P(x, t)$  including convective acceleration is given by

$$P(x, t) = M_m \cdot g_G \cdot \delta(x - v_M t) + M_m \cdot \ddot{w}_0(v_M t, t) \cdot \delta(x - v_M t), \quad (18)$$

( $M_m$ ) is the moving mass, ( $v_M$ ) is the traveling mass speed,  $\delta(\cdot)$  Is Dirac delta function, ( $g_G$ ) is the gravitational acceleration ( $g_G \approx 9.81 \text{ m/s}^2$ ), and ( $x$ ) is the abscissa, measured from the left end of the FGM beam. When ( $t = t_{Initial}$ ), the moving mass ( $M_m$ ) is in the left support of the beam whereas when ( $t = t_{Final}$ ), the mass ( $M_m$ ) just comes on the right support of the beam. The first and second terms of equation (18) are the virtual potential energy due to the weight and inertia of the moving mass, respectively.

## 6. Governing motion equations

The governing equilibrium equations of the present study can be obtained by integrating the derivatives by parts and replacing equations (14), (15) and (17) in equation (13):

$$\frac{\partial N^c}{\partial x} = I_1 \cdot \ddot{u}_0 - I_2 \cdot \ddot{w}_{0,x} + I_3 \cdot \ddot{\phi}_0, \quad (19)$$

$$\frac{\partial^2 M^c}{\partial x^2} = I_2 \cdot \ddot{u}_{0,x} - I_4 \cdot \ddot{w}_{0,xx} + I_5 \cdot \ddot{\phi}_{0,x} + I_1 \cdot \ddot{w}_0 + M_m \cdot (g_G + \ddot{w}_0(v_M t, t)) \cdot \delta(x - v_M t), \quad (20)$$

$$\frac{\partial M^{sd}}{\partial x} - Q = I_3 \cdot \ddot{u}_0 - I_5 \cdot \ddot{w}_{0,x} + I_6 \cdot \phi_0. \quad (21)$$

The variable separation approach is used to the discretization of the partial derivatives for the forced vibration problem in the spatial domain; as indicated by the following formulas:

$$u_0(x, t) = \sum_{j=1}^n \varphi_j(x) \cdot u_j(t), \quad (22)$$

$$w_0(x, t) = \sum_{k=1}^n \psi_k(x) \cdot w_k(t), \quad (23)$$

$$\phi_0(x, t) = \sum_{p=1}^n \phi_p(x) \cdot \phi_p(t), \quad (24)$$

where  $u_j(t)$ ,  $w_k(t)$  and  $\phi_p(t)$  are the temporary functions.  $\varphi_j(x)$ ,  $\psi_k(x)$  and  $\phi_p(x)$  are the shapes function associated respectively with the axial, transverse deflection and distortion fields of the functionally graded beams.  $(n)$  is the number of mode shape involved in the admissible functions. From Equation (23) we deduce the acceleration of the moving mass:

$$\ddot{w}_0(v_M t, t) = \sum_{k=1}^n \left( \psi_k(v_M t) \cdot \dot{w}_k(t) + 2 v_M \cdot \psi_{k,x}(v_M t) \cdot \dot{w}_k(t) + v_M^2 \cdot \psi_{k,xx}(v_M t) \cdot w_k(t) \right). \quad (25)$$

Introduce the equations (22, 23, and 24) into the government equations (19), (20) and (21), Multiply both sides respectively by  $\varphi_i(x)$ ,  $\psi_i(x)$  and  $\phi_i(x)$  ( $i = 1, 2, \dots, n$ ), integrating over the interval  $[0, L]$ , we obtain the following differential equations:

$$\begin{aligned} & \int_0^L \varphi'_i(x) \cdot \left( A_{11} \sum_{j=1}^n \varphi'_j(x) \cdot u_j(t) - B_{11} \sum_{k=1}^n \psi''_k(x) \cdot w_k(t) + E_{11} \sum_{p=1}^n \phi'_p(x) \cdot \phi_p(t) \right) dx \\ & + \int_0^L \varphi'_i(x) \cdot \left( I_1 \sum_{j=1}^n \varphi_j(x) \cdot \ddot{u}_j(t) - I_2 \sum_{k=1}^n \psi'_k(x) \cdot \ddot{w}_k(t) + I_3 \sum_{p=1}^n \phi_p(x) \cdot \ddot{\phi}_p(t) \right) dx = 0 \end{aligned} \quad (26)$$

$$\begin{aligned} & \int_0^L \psi''_i(x) \cdot \left( -B_{11} \sum_{j=1}^n \varphi'_j(x) \cdot u_j(t) + D_{11} \sum_{k=1}^n \psi''_k(x) \cdot w_k(t) - F_{11} \sum_{p=1}^n \phi'_p(x) \cdot \phi_p(t) \right) dx \\ & + \int_0^L \psi'_i(x) \cdot \left( -I_2 \sum_{j=1}^n \varphi_j(x) \cdot \ddot{u}_j(t) + I_4 \sum_{k=1}^n \psi'_k(x) \cdot \ddot{w}_k(t) - I_5 \sum_{p=1}^n \phi_p(x) \cdot \ddot{\phi}_p(t) \right) dx \\ & + \int_0^L \psi_i(x) \cdot \left( I_1 \sum_{j=1}^n \varphi_j(x) \cdot \ddot{u}_j(t) \right) dx + \int_0^L \psi_i(x) \cdot \left( M_m \sum_{j=1}^n \psi_k(v_M t) \cdot \ddot{w}_k(t) \right) \delta(x - v_M t) dx \\ & + \int_0^L \psi_i(x) \cdot \left( 2 M_m v_M \sum_{k=1}^n \psi_{k,x}(v_M t) \cdot \dot{w}_k(t) \right) \delta(x - v_M t) dx \\ & + \int_0^L \psi_i(x) \cdot \left( M_m v_M^2 \sum_{k=1}^n \psi_{k,xx}(v_M t) \cdot w_k(t) \right) \delta(x - v_M t) dx \\ & = - \int_0^L \psi_i(x) M_m \cdot g_G \cdot \delta(x - v_M t) dx \end{aligned} \quad (27)$$

$$\begin{aligned}
& \int_0^L \phi_i'(x) \cdot \left( E_{11} \sum_{j=1}^n \phi_j'(x) \cdot u_j(t) - F_{11} \sum_{k=1}^n \psi_k''(x) \cdot w_k(t) + H_{11} \sum_{p=1}^n \phi_p'(x) \cdot \varphi_p(t) \right) dx \\
& + \int_0^L \phi_i(x) \cdot \left( A_{55} \sum_{p=1}^n \phi_p(x) \cdot \varphi_p(t) \right) dx \\
& + \int_0^L \phi_i(x) \cdot \left( I_3 \sum_{j=1}^n \phi_j(x) \cdot \ddot{u}_j(t) - I_5 \sum_{k=1}^n \psi_k'(x) \cdot \ddot{w}_k(t) + I_6 \sum_{p=1}^n \phi_p(x) \cdot \ddot{\varphi}_p(t) \right) dx = 0
\end{aligned} \tag{28}$$

The Dirac delta function of the moving mass in the equation (27) is defined by Fryba [29]:

$$\int_0^L \psi_i(x) \cdot \delta^{(n)}(x - v_M t) \cdot dx = \begin{cases} -(1)^n \cdot \psi_i^n & \text{if } 0 < x_p < L \\ 0 & \text{Otherwise} \end{cases} \tag{29}$$

where  $\delta^{(n)}$  represents  $n$ -th derivative of the Dirac delta function. The secondary variables are turned to zero, the governing differential equation of the functionally graded beams under moving mass can be written in the general form:

$$[M(t)]\{\ddot{q}(t)\} + [C(t)]\{\dot{q}(t)\} + [K(t)]\{q(t)\} = \{F(t)\}, \tag{30}$$

where the transient mass matrices  $M(t)$ , transient damping matrices  $C(t)$ , and transient stiffness matrices  $K(t)$  are of order  $[3n \times 3n]$ , the temporary displacement vectors  $\{q(t)\}$  and temporary force vectors  $\{F(t)\}$  are of order  $[3n \times 1]$ . It should be noted that since the matrices  $M(t)$ ,  $C(t)$  and  $K(t)$  are updated at each time step, the moving mass problems take much longer than the moving load problems.

## 7. Numerical results and discussion

Numerical examples are presented and discussed under various parameters to verify the correctness of the current model as well as predict the dynamic responses of functionally graded material beams excited by a moving mass. In this section, simply supported beams are targeted by the functions (31, 32, and 33) which are assumed to be the modal shapes of the FGM beam. A mixture of steel and Alumina consists of FGM beam which the mechanical properties of each material are listed in Table 2. The material of the beam at the top end is pure alumina, whereas it is pure steel at the bottom end of the beam. The material properties change through the thickness direction of the beams according to exponential law function (E-FGM).

$$\varphi_j(x) = \cos\left(\frac{j \cdot \pi}{L} x\right) \quad (j = 1, 2, 3, \dots, n), \tag{31}$$

$$\psi_k(x) = \sin\left(\frac{k \cdot \pi}{L} x\right) \quad (k = 1, 2, 3, \dots, n), \tag{32}$$

$$\phi_p(x) = \cos\left(\frac{p \cdot \pi}{L} x\right) \quad (p = 1, 2, 3, \dots, n). \tag{33}$$

Table 1. Material properties of the functionally graded beam

Properties	Unit	Steel	Alumina
E	GPa	210	390
$\rho$	kg/m <sup>3</sup>	7800	3960
$\nu$	-	0.3	0.3

The governing differential equations of the dynamic system are solved numerically using Newmark average acceleration method via MATLAB calculator program, with uniform time increment. The normalized transverse dynamic deflection  $D(t)$  is calculated at the mid-span of the FG simply supported beam which gives maximum displacements, expressed by the following relation:

$$D(t) = \frac{w_d(L/2, t)}{w_s(L/2, t)}, \quad (34)$$

$w_x(L/2)$  is the static deflection of the full steel beam. A maximum normalized dynamic deflection is described by:

$$D_{\max} = \max(D(t)) = \max\left(\frac{w_d(L/2, t)}{w_s(L/2)}\right). \quad (35)$$

The forced dynamic responses are represented by two types of models, model A; without mass inertia effect and model B; with mass inertia effect. The mass values are normalized against the mass of the beam which is presented in terms of mass ratio  $M_{ratio} = M_M/M_{beam}$ . The initial time is considered by the starting time ( $t_{Initial} = 0$ ) and the final time  $t_{Final}$  is the total traveling time of the moving mass, presented by the symbol T ( $t_{Final} = T = \frac{L}{v_M}$ ). A parametric study was carried out to analyze the effect of; physical factors, speed and inertia of the moving mass, slenderness ratio, and mass ratio, on the modal responses.

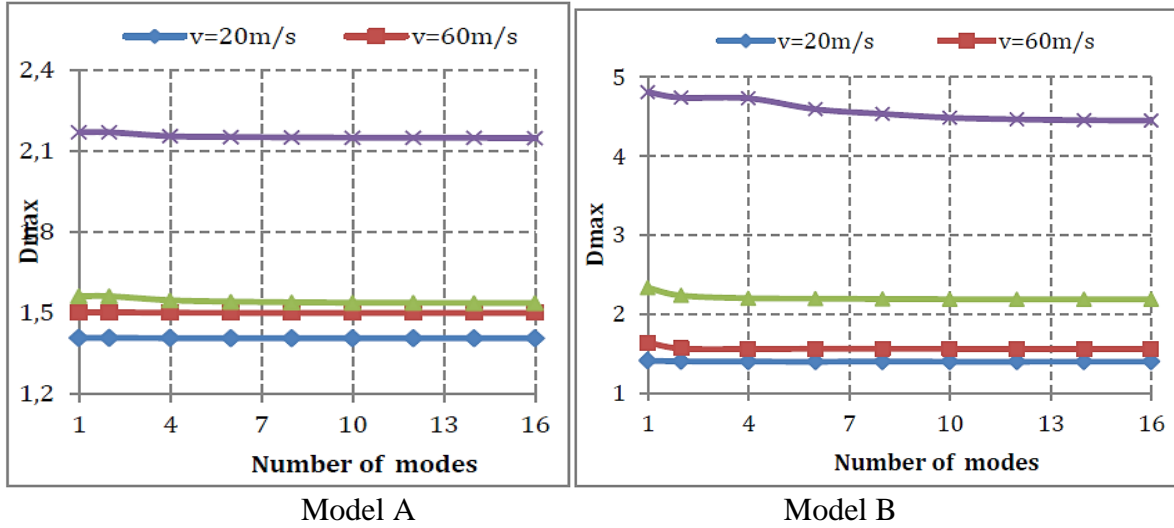


**Fig. 3.** Convergence study of maximum normalized dynamic deflection

The values of the maximum dynamic deflection ( $D_{\max}$ ) of the functionally graded beams as a function of the number of modes with/without mass inertia effect are shown in Fig. 3; by varying the displacement speed ( $v$ ), with  $L/h = 10$ . We observe that the results of  $D_{\max}$  stabilize from the use of several vibratory modes, regardless of the speed applied and the mathematical model is chosen. We can thus say that the response contribution of the higher modes to the dynamic deflection cannot be ignored. Consequently, for a satisfactory numerical precision in the subsequent calculations, the number of vibratory modes taken is fixed at eight (8) for model A and twelve (12) for model B.

The results of the fundamental frequencies and the dynamic shear correction factor are presented in Table 2 to validate the present shearing stress distribution and to predict the natural axial, bending, and shear frequencies for short and slenderness simply supported functionally graded beams. The dimensionless fundamental frequency ( $\varpi$ ) is defined as follows:

$$\varpi_m = \frac{\omega_m L^2}{h} \sqrt{\frac{\rho_b}{E_b}} \quad (36)$$

Upon examination of the table, it is revealed that the present eigenfrequencies and the dynamic shear correction factor agree with those presented by other researchers. This implies



that the present model is applicable in the dynamics of structures with success due to their simplicity and efficiency in complex formula systems.

Table 2. Validation of eigenfrequencies ( $\omega_m$ ) and dynamic shear correction factors (Kd)

Materials	Functions	Kd	L/h=5			L/h=20		
			$\omega_u$	$\omega_w$	$\omega_\phi$	$\omega_u$	$\omega_w$	$\omega_\phi$
	<b>Present</b>	<b>0.82268</b>	<b>31.494</b>	<b>5.3448</b>	<b>99.631</b>	<b>125.97</b>	<b>5.6865</b>	<b>1497.5</b>
	Thai et al.[30]	0.83747	31.494	5.3517	100.42	125.97	5.6870	1510.8
	Nguyen et al. [31]	0.82316	31.494	5.3447	99.658	125.97	5.6865	1498
	Pham and Vu [32]	0.82247	31.494	5.3451	99.617	125.97	5.6865	1497.4
FGM	<b>Present</b>	<b>0.82268</b>	<b>22.611</b>	<b>3.8184</b>	<b>72.993</b>	<b>90.915</b>	<b>4.0661</b>	<b>1090.5</b>
	Mantari et al. [33]	0.82314	22.611	3.8183	73.069	90.915	4.0661	1091.6
	Nguyen-Xuan et al. [34]	0.82878	22.614	3.8214	73.195	90.915	4.0663	1094.1
	Darijani and Mohammadabadi [35]	0.83969	22.617	3.8249	73.605	90.916	4.0666	1101.1
Full Steel	<b>Present</b>	<b>0.82268</b>	<b>16.466</b>	<b>2.7945</b>	<b>52.092</b>	<b>65.866</b>	<b>2.9732</b>	<b>782.99</b>
	Gandhe et al. [36]	0.82351	16.466	2.7945	52.117	65.866	2.9732	783.39
	Bedia et al.[37]	0.82546	16.466	2.7958	52.168	65.866	2.9733	784.3
	Ziou et al. [38]	0.82353	16.466	2.7945	52.117	65.866	2.9732	783.4

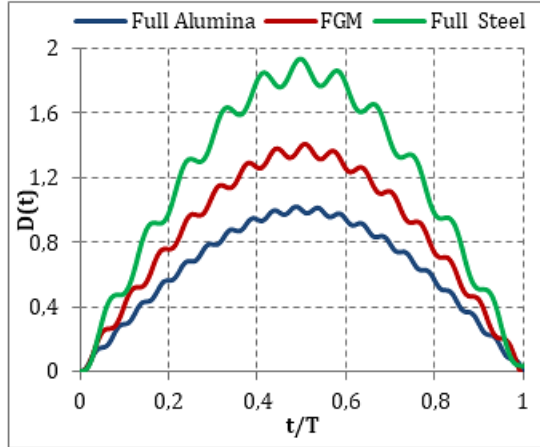
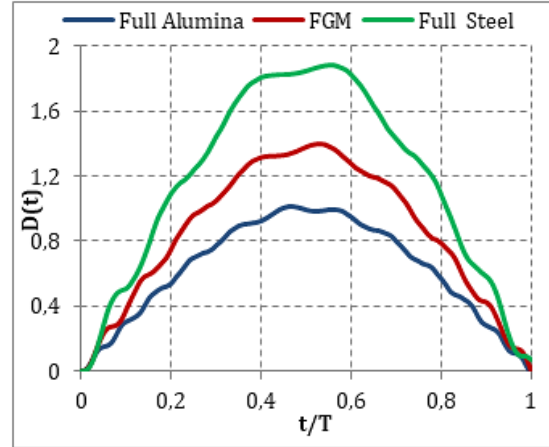
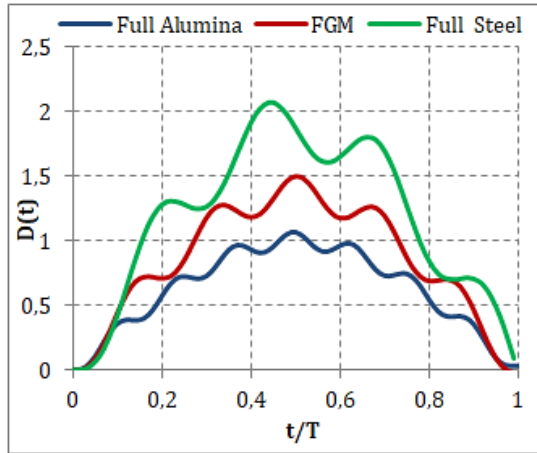
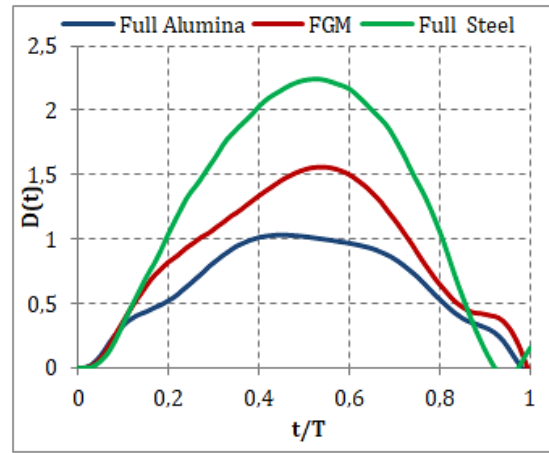
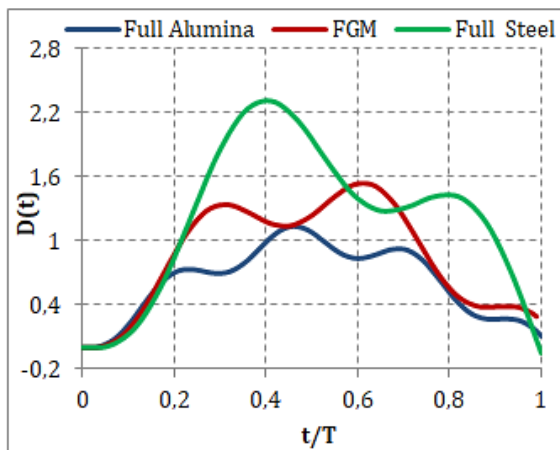
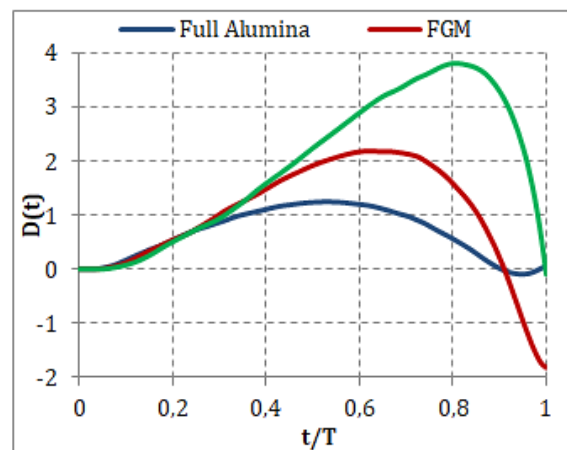
Table 3. Comparison of maximum normalized dynamic deflections

Model type	Materials	Maximum normalized dynamic deflections					
		$v_m = 20$ m/s		$v_m = 125$ m/s		$v_m = 250$ m/s	
		Present	Ref [39]	Present	Ref [39]	Present	Ref [39]
<b>Model A</b>	Full Alumina	<b>0.5610</b>	0.5656	<b>0.7537</b>	0.7852	<b>0.9327</b>	0.9321
	FGM	<b>0.7872</b>	0.7868	<b>1.1984</b>	1.2274	<b>1.2186</b>	1.1911
	Full Steel	<b>1.0970</b>	1.0993	<b>1.7277</b>	1.7316	<b>1.4163</b>	1.3825
<b>Model B</b>	Full Alumina	<b>0.5600</b>	0.5547	<b>0.8211</b>	0.8525	<b>1.0837</b>	1.0913
	FGM	<b>0.7699</b>	0.7701	<b>1.2823</b>	1.3107	<b>1.4400</b>	1.4161
	Full Steel	<b>1.0847</b>	1.0689	<b>1.8466</b>	1.8597	<b>1.5240</b>	1.5636

In Table 3, the maximum dynamic deflections are validated to numerical precedents available in the literature, with the corresponding speeds ( $v_m = 20$  m/s,  $v_m = 125$  m/s and  $v_m = 250$  m/s) for a span  $L = 20$  m, width  $b = 0.4$  m, thickness  $h = 0.9$  m, subjected to a mobile mass ( $M.g_G = 100$  kN) [39], while varying the materials properties of the Beams. For resent of compatibility, the static deflection at the middle of simply supported FG beam is presented in the form:

$$w_s\left(\frac{L}{2}\right) = -\frac{P.L^3}{48.E_b.I} \quad (37)$$

We see that the results obtained are very close to that obtained by Khalili et al. [39]. It is also noted that the  $D_{\max}$  is inversely proportional to the beam stiffness for the current model A and B. This implies that the material distribution plays a key role in changing the maximum transverse dynamic deflections of FGM beams.

Model A:  $v_m = 20$  m/sModel B:  $v_m = 20$  m/sModel A:  $v_m = 60$  m/sModel B:  $v_m = 60$  m/sModel A:  $v_m = 120$  m/sModel B:  $v_m = 120$  m/s

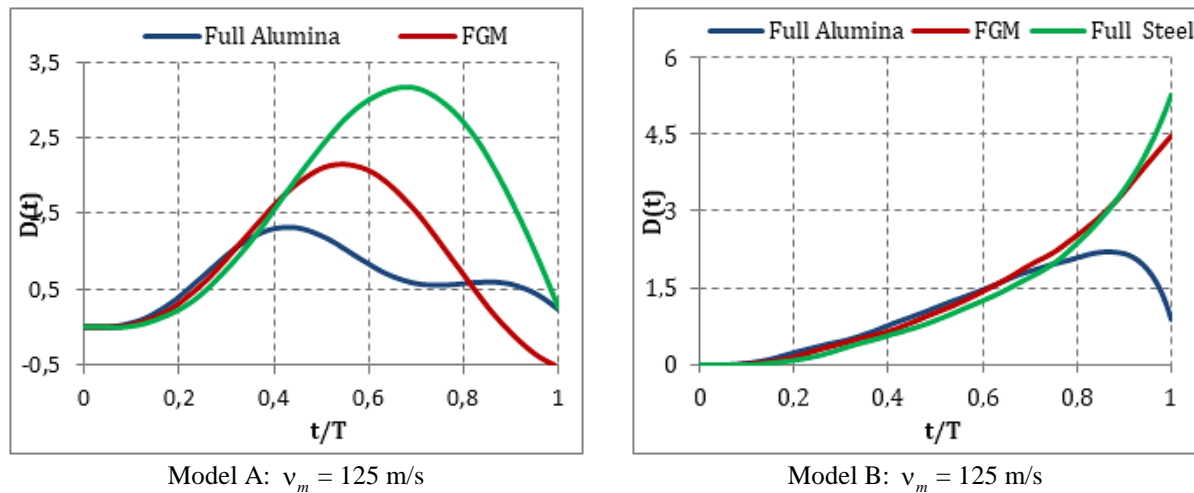


**Fig. 4.** Time histories for normalized mid-span dynamic deflection

In Figure 4, the time history of the normalized transverse dynamic deflection is shown by varying the material distributions of the FGM beam using two models A and B. The dynamic deflection is plotted under different speeds of the moving mass ( $v_m = 20$  m/s,  $v_m = 60$  m/s,  $v_m = 120$  m/s and  $v_m = 125$  m/s). We can see the inertia effect of the moving mass on the modal responses of the functionally graded beam; the dynamic shape of the moving load (model A) differs from that of the moving mass (model B). The maximum dynamic deflections obtained with consideration of the mass inertia effect are greater than those obtained without the mass inertia effect. This difference becomes large when the speed of the moving mass increases and thus negligible when the speeds of the moving mass decrease.

The physical factor of the beam has a favorable impact on the variation of the modal responses, the shape of the normalized dynamic deflection becomes highest when the beam is purely steel and minimum when the beam is purely alumina, regardless of the speed applied and the mathematical model proposed (A or B). For the FGM beam case, the dynamic response is optimal because the mechanical properties are a mixture of two basic materials, which depends on the combination of the volume fraction of the extreme materials (steel and alumina).

The dynamic system is strongly influenced by the speeds of the moving mass; increasing the moving charge speed gives stability to the vibratory behavior of the FGM beam, this is quite clear in model A. For low speeds ( $v = 20$  m/s), the dynamic deflection reacts similarly to an almost static beam.

The critical position of the moving mass which gives a significant dynamic deflection varies according to the values of the speeds, the maximum deflection moves in the middle towards the right end of the beam, which is remarkable in model B.

The mass ratio impact on the maximum dynamic deflections of the functionally graded beam is examined in figure 5 for various values of moving mass velocities. The calculation is carried out with a slenderness ratio  $L/h = 10, 20, 50$ , and  $100$ . It is observed that the increase in mass ratio does not always correspond to the highest amplitudes of the maximum normalized dynamic deflections, but it also depends on other secondary parameters such as; the slenderness ratio and the speed of the moving mass. The mass ratio is more pronounced at high velocity for FGM beams with small and medium aspect ratios.

Unlike modeling of long FGM beams, the mass ratio is affected when the moving mass is traversed at low or medium speeds. For a high velocity, the mass ratio effect is not significant because the maximum normalized dynamic deflections fall to values close to zero.

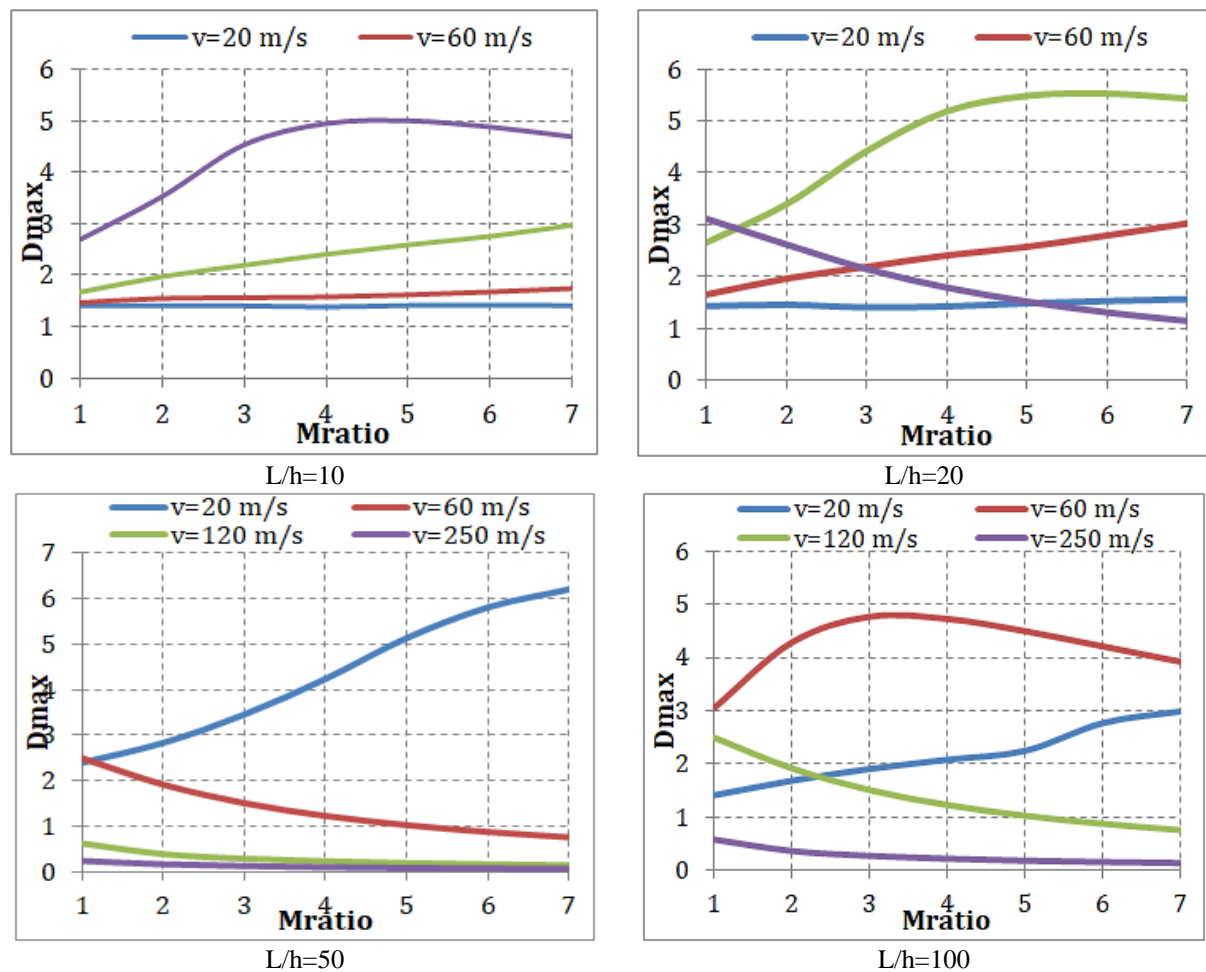


**Fig. 5.** Influence of mass ratio on maximum normalized dynamic deflections

## 8. Conclusion

The dynamic modeling of functionally graded (FG) beams traversed by a mobile mass is investigated, based on new Simple Fifth order Polynomial Shear Deformation Beam Theories (SFPSDBT). The material properties vary continuously through the thickness direction of the beam according to the exponential law function. The modal responses are determined by Newmark's temporal integration method via the MATLAB calculator program. The numerical results are converged and validated with those available in the literature. Several parameters have been described by numerous graphs and tables. The study showed that the dynamic behavior of forced vibrations is not only governed by the intrinsic parameter of the beam but also by the physical factors of the moving mass.

## References

- [1] Geronymos S. *Modélisation vibratoire en flexion de poutres composites multicouches à section creuse suite à un impact*. Montréal: Thèse de doctorat, école Polytechnique de Montréal; 2014.
- [2] Leissa AA. Direct method for analyzing the forced vibrations of continuous systems having damping. *Journal of Sound and Vibration*. 1978;56(3): 313-324.
- [3] El-Wazery MS, El-Desouky AR. A review on functionally graded ceramic-metal materials. *Journal of Materials and Environmental Science*. 2015;6(5): 1369-1376.
- [4] Celebi K, Yarimpabuc D, Keles I. A novel approach to thermal and mechanical stresses in a FGM cylinder with exponentially-varying properties. *Journal of Theoretical and Applied Mechanics*. 2017;55(1): 343-351.

- [5] Lee YH, Bae SI, Kim JH. Thermal buckling behavior of functionally graded plates based on neutral surface. *Composite Structures*. 2016;137: 208-214.
- [6] Apetre NA. *Sandwich panels with functionally graded core*. Florida: University of Florida; 2005.
- [7] Zhang DG, Zhou HM. Mechanical and thermal post-buckling analysis of FGM rectangular Plates with various supported boundaries resting on nonlinear elastic foundations. *Thin-Walled Structures*. 2015;89: 142-151.
- [8] Bouamama M, Refassi K, Elmeiche A, Megueni A. Dynamic Behavior of Sandwich FGM Beams. *Mechanics and Mechanical Engineering*. 2018;22(4): 919-930.
- [9] Garg A, Belarbi, MO, Chalak HD, Chakrabarti A. A review of the analysis of sandwich FGM structures. *Composite Structures*. 2020;258: 113427.
- [10] Elhannani A, Refassi K, Elmeiche A, Bouamama, M. Vibration analysis of functionally graded tapered rotor shaft system. *Mechanics and Mechanical Engineering*. 2019;23(1): 241-245.
- [11] Hassan Ahmed Hassan A, Kurgan N, Can N. The Relations between the Various Critical Temperatures of Thin FGM Plates. *Journal of Applied and Computational Mechanics*. 2020;6: 1404-1419.
- [12] Ebrahimi F, Ghasemi F, Salari E. Investigating thermal effects on vibration behavior of temperature-dependent compositionally graded Euler beams with porosities. *Meccanica*. 2015;51(1): 223-249.
- [13] Nami MR, Janghorban M. Resonance behavior of FG rectangular micro/nano plate based on nonlocal elasticity theory and strain gradient theory with one gradient constant. *Composite Structures*. 2014;111: 349-353.
- [14] Bendine K, Boukhoulda BF, Nouari M, Satla Z. Structural modeling and active vibration control of smart FGM plate through ANSYS. *International Journal of Computational Methods*. 2017;14(04): 1750042.
- [15] Bendine K, Boukhoulda BF, Nouari M, Satla Z. Active vibration control of functionally graded beams with piezoelectric layers based on higher order shear deformation theory. *Earthquake Engineering and Engineering Vibration*. 2016;15(4): 611-620.
- [16] Ng T, Lam K Y, Liew K. Effects of FGM materials on the parametric resonance of plate structures. *Computer Methods in Applied Mechanics and Engineering*. 2000;190(8-10): 953-962.
- [17] Khebizi M, Hamza G, Guenfoud M, El Fatmi R. Three-dimensional modelling of functionally graded beams using Saint-Venants beam theory. *Structural Engineering and Mechanics*. 2019;72(2): 257-273.
- [18] Majak J, Shvartsman B, Ratas M, Bassir D, Pohlak M, Karjust K, Eerme M. Higher-order Haar wavelet method for vibration analysis of nanobeams. *Materials Today Communications*. 2020;25: 101290.
- [19] Garg A, Chalak HD, Chakrabarti A. Comparative study on the bending of sandwich FGM beams made up of different material variation laws using refined layerwise theory. *Mechanics of Materials*. 2020;151.
- [20] Lee JW, Lee JY. Free vibration analysis of functionally graded Bernoulli-Euler beams using an exact transfer matrix expression. *International Journal of Mechanical Sciences*. 2017;122: 1-17.
- [21] Huang Y, Lu HW, Fu JY, Liu AR, Gu M. Dynamic Stability of Euler Beams under Axial Unsteady Wind Force. *Mathematical Problems in Engineering*. 2014;1-12. Available from: [doi.org/10.1155/2014/434868](https://doi.org/10.1155/2014/434868).
- [22] Mohanty SC, Dash RR, Rout T. Static and dynamic stability analysis of a functionally graded Timoshenko beam. *International Journal of Structural Stability and Dynamics*. 2012;12(04): 1250025.

- [23] Bouamama M, Elmeiche A, Elhennani, A, Kebir T. Dynamic Stability Analysis of Functionally Graded Timoshenko Beams with Internal Viscous Damping Distribution. *Journal Européen des Systemes Automatisées*. 2019;52(4): 341-346.
- [24] Simsek M, Kocaturk T. Free and forced vibration of a functionally graded beam subjected to a concentrated moving harmonic load. *Composite Structures*. 2009;90(4): 465-473.
- [25] Almbaidin AA, Abu-Alshaukh, IM. Vibration of functionally graded beam subjected to moving oscillator using Caputo-Fabrizio fractional derivative model. *Romanian Journal of Acoustics and Vibration*. 2019;16(2): 137-146.
- [26] Elmeiche A, Bouamama M, Megueni A. Dynamic analysis of FGM nanobeams under moving load considering shear deformation effect. *International Journal of Scientific & Engineering Research*. 2018;9(3): 1212-1221.
- [27] Nguyen DK, Thom TT, Gan BS, Van Tuyen B. Influences of dynamic moving forces on the functionally graded porous nonuniform beams. *International Journal of Engineering and Technology Innovation*. 2016;6(3): 173.
- [28] Delale F, Erdogan F. The crack problem for a nonhomogeneous plane. *Journal of Applied Mechanics*. 1983;50(3): 609-614.
- [29] Fryba L. *Vibration of Solids and Structures Under Moving Loads*. Groningen: Noordhoff Int Publish; Springer Science & Business Media. 1972:13-43.
- [30] Thai CH, Ferreira AJM, Bordas SPA, Rabczuk T, Nguyen Xuan H. Isogeometric analysis of laminated composite and sandwich plates using a new inverse trigonometric shear deformation theory. *European Journal of Mechanics-A/Solids*. 2014;43: 89-108.
- [31] Nguyen TK, Nguyen TTP, Vo TP, Thai HT. Vibration and buckling analysis of functionally graded sandwich beams by a new higher-order shear deformation theory. *Composites Part B: Engineering*. 2015;76: 273-285.
- [32] Phuc PM, Thanh VN. A new Sinusoidal Shear Deformation Theory for Static Bending Analysis of Functionally Graded Plates Resting on Winkler-Pasternak Foundations. *Advances in Civil Engineering*. 2020. Available from: doi.org/10.1155/2021/6645211.
- [33] Mantari J, Oktem AS, Soares CG. A new trigonometric shear deformation theory for isotropic, laminated composite and sandwich plates. *International Journal of Solids and Structures*. 2012;49(1): 43-53.
- [34] Nguyen Xuan H, Thai Chien H, Nguyen Thoi T. Isogeometric finite element analysis of composite sandwich plates using a higher order shear deformation theory. *Composite Part B*. 2013;55: 558-574.
- [35] Darijani H, Mohammadabadi H. A new deformation beam theory for static and dynamic analysis of microbeams. *International Journal of Mechanical Sciences*. 2014;89: 31-39.
- [36] Gandhe GR, Pankade PM, Tupe DH, Taur PG. Higher Order Computational Method for Static Flexural Analysis of Thick Beam. *Procedia Manufacturing*. 2018;20: 493-498.
- [37] Bedia WA, Houari MSA, Bessaim A, Bousahla AA, Tounsi A, Saeed T, Alhodaly MS. A new hyperbolic two-unknown beam model for bending and buckling analysis of a nonlocal strain gradient nanobeams. *Journal of Nano Research*. 2019;57: 175-191.
- [38] Ziou H, Guenfoud M, Guenfoud H. A Simple Higher-order Shear Deformation Theory for Static Bending Analysis of Functionally Graded Beams. *Jordan Journal of Civil Engineering*. 2021;15(2).
- [39] Khalili SMR, Jafari AA, Eftekhari SA. A mixed Ritz-DQ method for forced vibration of functionally graded beams carrying moving loads. *Composite Structures*. 2010;92(10): 2497-2511.

## THE AUTHORS

**Elmeiche A.**

e-mail: abbes.elmeiche@univ-sba.dz

ORCID: 0000-0002-1838-3105

**Bouamama M.**

e-mail: bouamamamohameddoc@gmail.com

ORCID: 0000-0003-1804-9091

**Elhannani A.**

e-mail: aze.atiu@hotmail.com

ORCID: 0000-0002-8964-4632

**Belaziz A.**

e-mail: belaziz2013@gmail.com

ORCID : 0000-0002-4737-753X

**Hammoudi A.**

e-mail: merzouk01@gmail.com

ORCID: 0000-0001-8911-348X